CrossMark

ORIGINAL PAPER

Cellulose fiber size defines efficiency of enzymatic hydrolysis and impacts degree of synergy between endo- and exoglucanases

Vanessa O. A. Pellegrini · Amanda Bernardes · Camila A. Rezende · Igor Polikarpov

Abstract An interplay between cellulases is fundamental in biomass saccharification. Here, the synergistic action of *Trichoderma harzianum* Cel7A and Cel7B on two cellulosic substrates: bacterial cellulose (BC) and a much more heterogeneous filter paper (FP) was investigated by determining their saccharification yields and by analyzing both the released soluble products and the insoluble reducing ends formed in the process. Furthermore, morphological changes of the substrates were evaluated using scanning electron microscopy. Glycoside hydrolase family 7 (GH7) enzymes introduce uniform changes in BC, whereas in FP they preferentially consume thin microfibrils rather than thicker paper fibers. Thus, the size effect, which leads to a smaller surface area per unit of substrate mass for thicker fibers, seems to play a crucial role in higher enzymatic hydrolysis efficiency of BC as compared to FP. These results demonstrate that the morphology-dependent effects could be essential for the industrial breakdown of cellulose-rich plant biomass.

V. O. A. Pellegrini · A. Bernardes · I. Polikarpov (✉)
Department of Physics and Interdisciplinary Science, São Carlos Institute of Physics, University of São Paulo, Av. Trabalhador Sãocarlense, 400, São Carlos, SP 13566-590, Brazil
e-mail: ipolikarpov@ifsc.usp.br

C. A. Rezende
Institute of Chemistry, University of Campinas, P.O. Box 6154, Campinas, SP 13083-970, Brazil

Introduction

Lignocellulosic biomass is the most abundant source of renewable biopolymers on Earth and a promising renewable feedstock for the production of cellulosic ethanol and green chemicals. The sustainable use of lignocellulosic residues contributes to reduce pollutant gas emissions, to reach a profitable use of agricultural waste and to enhance the bioethanol productivity (Ganner et al. 2012).

The bioconversion of lignocellulose to fuels and chemicals generally involves several technological steps such as pretreatment, enzymatic hydrolysis, and fermentation (Ganner et al. 2012; Kostylev and Wilson 2014) and costs of the enzymes is is currently one of the major factors which impacts economic viability of these nascent technologies. Therefore, the development of enzymatic mixtures capable of overcoming the heterogeneity and the recalcitrance of plant cell walls in a cost-efficient manner represents a

major technological challenge in sustainable ligno-cellulose utilization.

Over the years, the early model of cellulose hydrolysis proposed by Reese et al. (1950) has been significantly extended and detailed as more information on the roles and specificities of enzymes involved in cellulose degradation became available. The simplest set of cellulolytic enzymes involved in cellulose depolymerization includes endoglucanases (EGs; endo-1,4-β-D-glucanase), cellobiohydrolases (CBHs; exo-1,4-β-D-glucanase) and β-glucosidases (1,4-β-D-glucosidase) (Serpa and Polikarpov 2011; Payne et al. 2015), although it becomes increasingly clear that other enzymes, such as lytic polysaccharide monooxigenases (LPMOs), for example, play an important role in degradation of this recalcitrant polysaccharide (Horn et al. 2012; Hemsworth et al. 2015).

The synergistic cooperation of different cellulases is essential for degradation of cellulose (Arantes and Saddler 2010). According to the classical model of cellulose hydrolysis, a synergism occurs between randomly acting EGs, which predominantly hydrolyze amorphous parts of cellulose, producing new termini in the cellulose chains that serve as starting points for the attack by the processive CBHs (known as endo–exo synergy). Thus, the classical model of endo–exo synergism is based on the notion that the chain-end availability is the major rate-limiting step for CBHs and when EGs are added, they generate new cellulose chain termini and consequently increase the population of productively bound CBHs and, consequently, an overall hydrolysis yield. However, a standout study of Kurasin and Väljamäe (2011) on *T. reesei* Cel7A showed that the rate of cellulose hydrolysis is limited by the slow dissociation of the trapped CBHs, which can be rescued by *T. reesei* endoglucanases. It has been demonstrated that *Tr*Cel7Bs (and also *Tr*Cel6As) are capable of facilitating the release of unproductively bound *Tr*Cel7As stuck at the amorphous regions of cellulosic substrates (Kurasin and Väljamäe 2011; Igarashi et al. 2011; Jalak et al. 2012). Thus, the synergistic effect mostly results from the increase in the rate constant of cellulose hydrolysis, and not only from alleviating restriction on the number of reducing chain ends available for Cel7A recognition (Jalak et al. 2012; Kuusk et al. 2015). Lately, the importance of accessory enzymes and the synergism between

cellulases and proteins with auxiliary activities (such as LPMOs) has also been recognized (Harris et al. 2010; Vaaje-Kolstad et al. 2010; Horn et al. 2012; Payne et al. 2015).

For cellulase mixtures, a synergism could be defined as a cooperative enhancement of joint activity of different types of cellulases acting together, where the activity of the mixture is higher than the sum of the activity of each individual enzyme (Kostylev and Wilson 2012). Quantitative description of synergism is often described in terms of a degree of synergy (DS), defined as the ratio between the activity of the synergistic mixture and the sum of the activities of individual components (Zhang and Lynd 2004; Jeoh et al. 2006; Jalak et al. 2012). DS is affected by many parameters, such as nature, morphology, and accessible area of the substrate (Watson et al. 2002; Zhang and Lynd 2004; Kostylev and Wilson 2012); a molar ratio of the components and total enzyme loadings (Boisset et al. 2001) and also reaction time (Väljamäe et al. 1999; Boisset et al. 2001; Jeoh et al. 2006).

Since different degrees of synergism can be associated with the substrates and the experimental conditions used, the synergistic properties of cellulases have been investigated against different substrates (Kostylev and Wilson 2012). The most common model substrates used for synergism studies are phosphoric acid swollen cellulose (PASC), filter paper (FP), Avicel, and bacterial cellulose (BC). The two substrates selected for the present study, FP and BC, differ in their physical and chemical properties, such as morphology, average degree of polymerization (DP_N) and crystallinity (Zhang and Lynd 2004). BC has significantly higher DP_N than FP (2000 and 750, respectively; Zhang and Lynd 2004). Furthermore, it has been reported that dried BC is more crystalline than FP (Zhang and Lynd 2004). It is important to notice, however, that degree of crystallinity estimates vary with an applied physical technique and a method of evaluation (Zhang and Lynd 2004; Bernardinelli et al. 2015).

Normally, DS between cellulases is reduced for the more crystalline materials (Väljamäe et al. 1999; Jeoh et al. 2006). For example, Henrissat et al. (1985), after assaying FP, Avicel, BMCC and Valonia microcrystals using combinations of *Trichoderma reesei* enzymes, did not observed any synergism in Valonia cellulose enzymatic degradation, which is a highly crystalline material.

An important parameter of cellulase action is the processivity, which is defined as an average number of catalytic cleavages carried out by an enzyme on a cellulose chain before their dissociation (Wilson and Kostylev 2012). A highly processive CBH, which releases a large number of cellobiose molecules from the cellulosic substrate per binding-dissociation cycle, would be expected to generate a much higher number of soluble than insoluble reducing ends. On the other hand, an ideal EG is expected to produce new cuts in the amorphous regions of the cellulose chains at random sites in a non-processive way, thus generating mostly insoluble termini along with a small amount of soluble saccharides. Though CBHs mostly act processively on the available cellulose chain termini of the crystalline substrate (Kostylev and Wilson 2012), they are also capable of initiating the attack in an endocellulase manner (Ståhlberg et al. 1993; Boisset et al. 2000; Kurasin and Väljamäe 2011; Jalak et al. 2012; Badino et al. 2017).

To the best of our knowledge, the synergism between *Trichoderma harzianum* endoglucanase I (*Th*Cel7B) and cellobiohydrolase I (*Th*Cel7A) has not been studied before. Here we set out to investigate the enzymatic hydrolysis of well-defined model substrates with different polymerization, crystallinity and morphology, FP and BC, by these enzymes independently and in combination. To better analyze the contributions of each enzyme to the observed synergism and to estimate their processivity, the release of reducing ends by *Th*Cel7A and *Th*Cel7B in the supernatant and the reducing sugar ends generated in insoluble substrate were measured, as described by Silveira et al. (2014). Differently from the commonly used DNS assay that provides the total amount of reducing sugars only (Miller 1959), the approach applied here allows to evaluate individual and combined enzymatic action on cellulosic substrates by measuring amounts of both soluble and insoluble reducing ends. Furthermore, scanning electron microscopy was used to visualize structural changes in the substrates subjected to the enzymatic depolymerization. *Th*Cel7B and *Th*Cel7A from the same glycoside hydrolase family 7 (GH7) were investigated to contribute to the development of more complete models for GH7 enzymatic degradation of the cellulosic substrates.

Materials and methods

Substrates

Activities of the enzymes were determined on both filter paper (FP) and bacterial cellulose (BC). The FP used was Whatman No. 1 (GE Healthcare Biosciences, Little Chalfont, UK) that is made out of cotton cellulose and widely applied for determination of the international Filter Paper Units (FPU) of enzymatic activity (Payne et al. 2015). The BC was produced using *Gluconacetobacter hansenii* ATCC 23769 strain (GenBank number: CM000920), following a procedure described in a literature (Chawla et al. 2009). Briefly, the bacteria were grown in modified HS medium (Schramm and Hestrin, 1954), containing 25 g L^{-1} of D-mannitol, 5 g L^{-1} of yeast extract, 3 g L^{-1} of peptone, with pH = 6.0, and statically incubated at 30 °C for 45 days. The cellulose membrane produced was recovered, washed with deionized water to remove the residual culture medium and treated with 0.1 M NaOH at 80 °C for 20 min. To neutralize the medium, 5% acetic acid solution was applied to BC, followed by rinsing with distilled water. Finally, the BC sheets were dried for 1 day and cut in a disc shape (⌀ = 5 mm).

Measurements of substrate crystallinities

Measurements of FP and BC crystallinity indices (CIs) were conducted using X-ray diffraction (XRD) technique. The XRD patterns were recorded on Miniflex 600 (Rigaku, Japan) instrument, using Cu Kα radiation (λ = 1.5406 Å) at ambient temperature. The XRD equipment was set to operate at 40 kV and 15 mA and 2θ scans were measured from 5 to 50° in 0.05 degree steps with an X-ray exposure of 15 s per step.

To calculate the CIs of the samples from the experimental XRD spectra, individual diffraction peaks were extracted by a curve-fitting process from the experimental diffraction scans. Peak fitting program (PeakFit; www.systat.com) was used to assume Gaussian functions for each peak and a broad background distribution with maximum at around 21.5° was assigned to the amorphous scattering contribution, as described by Park et al. (2010).

Enzymes

Trichoderma harzianum Cel7A and Cel7B (*Th*Cel7A and *Th*Cel7B, respectively), both heterologously expressed in *Aspergillus niger* were used in this study. *Th*Cel7B was cloned in *A. niger* and its production has been described previously (Pellegrini et al. 2015). *Th*Cel7A was produced following the same protocol. In short, the gene identified as "transcript ID 20062" was amplified from a cDNA library of *T. harzianum* IOC-3844, obtained from Instituto Oswaldo Cruz Culture Collection of Filamentous Fungi (CCFF; http://ccff.fiocruz.br/); cloned into a vector ANip7G (Storms et al. 2005), using the Gateway technology (Katzen 2007) and transformed in *Aspergillus niger*, as described (Pellegrini et al. 2015). Positive transformants were inoculated in 2 L erlenmeyer flasks containing 500 mL of minimal medium with maltose as a carbon source. The growth step was carried out at 30 °C over 6 days, under static condition. The purification started with overnight precipitation by ammonium sulfate at 80% saturation, followed by injection of protein in hydrophobic chromatography on a Phenyl-Sepharose 6 Fast Flow column (GE Healthcare Biosciences, Little Chalfont, UK), previously equilibrated with a 50 mM sodium citrate buffer (pH 5.0) and supplemented with a 1 M ammonium sulfate. The final purification step was accomplished by molecular exclusion chromatography, using a Superdex 75 16/60 column. Purities of the protein samples were analyzed by 15% SDS-PAGE and the enzyme identities were confirmed by mass spectrometry measurements.

Enzymatic assays: determination of optimal conditions

The most widely accepted model of synergism assumes that the molar ratios of the enzymes in mixtures influence the hydrolysis rate (Kostylev and Wilson 2012). To define the concentration and the molar ratios of the enzymes to be used in these experiments, different concentrations of *Th*Cel7A and *Th*Cel7B were tested.

Cellulase activities were defined in terms of Filter Paper Units (FPU) per grams of substrate (FPU/g), according to the International Union of Pure and Applied Chemistry (IUPAC), using a small amount of substrate (2.5 mg of FP). The FPU activity was determined for both *Th*Cel7B and *Th*Cel7A by incubation of different concentrations of purified enzymes in a 50 mM sodium citrate buffer (pH 5.0), with a 5.0 mm disc of Whatman No. 1 FP (2.5 mg), during 1 h. The reaction was stopped after addition of 100 μL of 3,5-dinitrosalicylic acid solution (DNS) by keeping the mixture at 100 °C for 5 min. Absorbance of the supernatant was measured at 540 nm and the assays were carried out in triplicate. Most of the enzymatic reactions were set up to contain the same cellulase load (fixed at 0.15 FPU/g of substrate) and the reaction periods of 0.25, 1.0, 2.0, 3.0, 6.0, 24 and 48 h were tested. For soluble, insoluble and total reducing sugars assays the enzyme concentration used was three times higher to assure that the soluble enzymatic products could be quantified. To certify that the enzymes were stable during the incubation periods, their residual activities were measured for the duration of the whole experiment.

Enzymatic assays using FP and BC: soluble, insoluble and total reducing ends production

To analyze total, soluble and insoluble reducing ends produced in the enzymatic hydrolysis, we have applied a method developed by Silveira et al. (2014) with adjustments concerning the reaction volume. The insoluble reducing ends (RS_{insol}) consist of reducing chain ends of cellulose microfibrils that remain attached to the cellulose. On the other hand, soluble reducing sugars (RS_{sol}) are the reducing ends of the soluble oligosaccharides released during enzymatic hydrolysis and the total reducing sugars (RS_{tot}) are the sum of both RS_{insol} and RS_{sol}. Experimentally, RS_{tot} and RS_{sol} are determined, while RS_{insol} is calculated by subtracting RS_{sol} from RS_{tot} (Silveira et al. 2014). The reactions were composed by 360 nM *Th*Cel7B and 780 nM *Th*Cel7A diluted in 200 μL of a 50 mM sodium citrate buffer (pH 5.0), supplemented with two 0.5 cm discs of Whatman No. 1 FP (5 mg). The same amount of substrate (5 mg) was used in experiments with BC. After 24 h, the total amount of reducing ends was determined using the supernatant and the residual substate, while the amount of soluble sugars was determined in the supernatant only, which was transferred to separate tubes. The aliquots were boiled with DNS and the absorbances were

determined spectroscopically at 540 nm, as described above.

Effect of pH on the synergy between GH7 cellulases

The optimal pH for *Th*Cel7B activity is 3 (Pellegrini et al. 2015), whereas *Th*CE7A is most active at pH 5 (Colussi et al. 2011). Therefore, as a first step, enzymatic activities of each individual *T. harzianum* enzyme and also of their their mixtures were evaluated at pHs 3, 4 and 5. Aiming to reach a final enzyme load of 0.15 FPU/g substrate when using the enzymes separately, the reaction medium was composed of 10 μL of enzyme diluted in 50 mM of sodium citrate buffer, corresponding to 260 nM of *Th*Cel7A or 120 nM of *Th*Cel7B, supplemented with a disc of Whatman nº 1 FP weighting 2.5 mg. In the studies of sinergism, the experimental conditions were kept the same, but the two enzymes were added together, while keeping the same enzyme load of 0.15 FPU/g substrate. In the negative control samples, the buffer substituted the enzyme volume. The mixture was incubated at 50 °C for 24 h, followed by the addition of 100 μL of DNS, and boiling at 100 °C for 5 min (without removing the FP). The absorbance of the solution was measured at 540 nm. Control reactions with the enzymes replaced by bovine serum albumin (BSA) were also carried out to check the influence of a model protein load upon the measured activity.

Morphological studies using field emission scanning electron microscopy (FESEM)

Morphological changes caused by the enzyme action on FP and BC were investigated using FESEM. Investigated substrates consisted either of a disc of Whatman No. 1 FP or a disc of BC, both weighting 2.5 mg. The substrates underwent hydrolysis for 12, 24 and 48 h, at 50 °C and pH 5.0, under a constant stirring rate of 1500 rpm. The assays were carried out in triplicate on the samples treated with *Th*Cel7A or *Th*Cel7B individually, or in a combination, as described above. The solid substrate recovered from the reaction was dried at 30 °C for 12 h, fixed in suitable stubs with carbon tape and then coated with a thin Au layer (ca. 16 nm) in a SCD 050 sputter coater (Oerlikon-Balzers, Balzers, Liechtenstein).

Secondary electron images were obtained under vacuum, using a 5 kV acceleration voltage in a scanning electron microscope equipped with a field emission gun (FESEM-FEI Quanta 650) at the Brazilian National Laboratory of Nanotechnology (LNNano; Campinas, SP, Brazil). For each sample, 8–10 different areas were analyzed in two replicates under 5–6 different magnifications. A total of 620 images were obtained from FP and BC samples to assure the repeatability and the reproducibility of the results.

Fiber diameters and areas in FESEM images were measured in the Image J free software (Schneider et al. 2012). The total surface occupied by voids in the samples before and after enzymatic hydrolysis was estimated by measuring the area of the voids in 4 different images of 0.31 mm^2 for each sample.

Results and discussion

Enzymatic assays settings and synergy between *Th*Cel7A and *Th*Cel7B

The temporal variation in the hydrolysis yields was assessed by quantifying the product reducing ends released in the hydrolysate after different reaction times of 0.25, 1, 2, 3, 6, 24 and 48 h (Figure ESM1). The enzymatic loads of *Th*Cel7A and *Th*Cel7B used here were chosen to highlight the effects of synergism between these enzymes, and not to maximize the amounts of enzymatic hydrolysis products. The enzyme concentration and the enzyme to substrate ratio influence the hydrolysis rates (Henrissat et al. 1985; Watson et al. 2002; Jeoh et al. 2006), and previous studies showed that the synergism tends to be stronger under lower enzymatic loads (Woodward et al. 1988).

The hydrolysis of FP by both enzymes followed a hydrolysis profile typical of cellulases, with an initial fast rate, followed by a gradual decrease until reaching a plateau. Under these experimental conditions, the exoglucanase activity becomes higher than the endoglucanase activity after approximately 6 h of hydrolysis, and for both enzymes, the cellulose hydrolysis starts to level off after 24 h (Figure ESM1). For this reason, 24 h was the hydrolysis time chosen for the initial experiments. A significantly enhanced hydrolytic activity is observed on FP when EG

*Th*Cel7B and CBH *Th*Cel7A are applied together (Fig. 1a), which is a consequence of their cooperative action. *T. harzianum* cellulases act synergistically, so that the glucose released by their mixture (0.59 μmol) is ca. 18% higher than the sum of the separate activities (0.50 μmol). BSA was used in the same concentration as a control to evaluate the effect of nonspecific interactions caused by the addition of a nonhydrolytic protein. For both cellulases, BSA addition showed very small and experimentally non-significant effect on the total saccharification yields (Fig. 1a).

The amounts of soluble and insoluble reducing ends released by each enzyme from FP were similar, with *Th*Cel7A releasing higher amount of soluble reducing ends (63%) as compared to *Th*Cel7B (54%), and *Th*Cel7B releasing more insoluble reducing ends as compared to *Th*Cel7A (46 and 37%, respectively) (Table 1). For BC, the enzymatic hydrolysis profile based on reducing sugar release is very different for both enzymes acting individually. *Th*Cel7B produced significantly higher amount of insoluble reducing ends (around 70%) and *Th*Cel7A presented predominantly soluble reducing ends (also around 70%) (Table 1).

The low ratios of soluble-to-insoluble reducing ends produced by separated cellulases on both substrates indicate that they have low apparent processivity. It is expected that a true endoglucanase would produce 30–40% of insoluble reducing ends from FP (Li et al. 2007; Kostylev and Wilson 2012), whereas *Th*Cel7B generates around 46% of insoluble reducing ends on FP and 72% in BC.

Notably, the simultaneous action of both *Th*Cel7A and *Th*Cel7B showed marked increase in soluble products in both substrates, which reached over 90% of the total released reducing ends (Table 1). This result reveals that practically all the reducing ends available on the substrates are consumed under the cooperative action of *Th*Cel7A and *Th*Cel7B and the apparent degree of processivity increases substantially when the two enzymes are acting together.

The relatively low ratio of soluble-to-insoluble reducing ends generated by *Th*Cel7A from the cellulosic substrates studied in the current work might seem somewhat surprising, considering the much higher expected processivity observed for typical exoglucanases, which are able to produce more than 90% of the total soluble reducing ends (Kurasin and Väljamäe 2011; Kostylev and Wilson 2012; Cruys-Bagger et al. 2013). However, recent X-ray crystallographic and molecular dynamics studies of *Th*Cel7A enzyme demonstrated its higher flexibility, as compared to the classical *T. reesei* Cel7A (Textor et al. 2013). Furthermore, molecular dynamics simulations of *Th*Cel7A revealed that this enzyme is capable of opening up large loops forming a catalytic tunnel of the enzyme, thus facilitating its dissociation from the crystalline substrate and the product release, and indicating its low processivity (Textor et al. 2013). This is consistent with the relatively small amounts of soluble sugars released by the enzyme as determined in the current experiments.

Moreover, the smaller fraction of the soluble reducing ends released by *Th*Cel7A from FP as compared to BC is consistent with the notion that, in
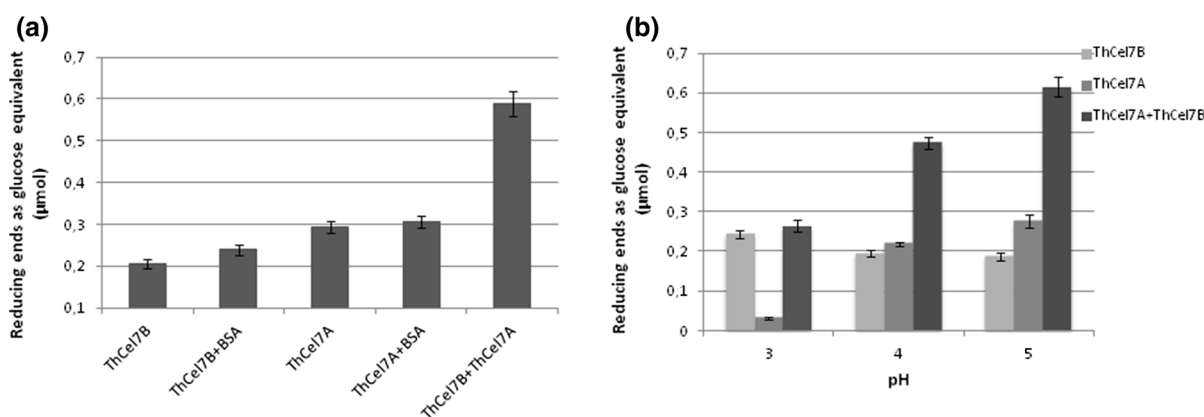

Fig. 1 Reducing ends as glucose equivalent (μmol) released from filter paper after 24 h of hydrolysis by *Th*Cel7B and *Th*Cel7A acting individually or in combination: **a** at pH = 5 and in the presence of BSA (controls); **b** under different pH conditions

Table 1 Percentages of soluble, insoluble reducing sugars released and substrate consumption by the endoglucanase *Th*Cel7B (120 nM) and the cellobiohydrolase *Th*Cel7A (260 nM) acting individually or in combination on FP (5 mg) or BC (5 mg)

Substrate	Enzymes	Reducing sugar (% of the total)		Substrate consumption (%)		
		Soluble	Insoluble	Soluble fraction	Insoluble fraction	Total
Filter paper	*Th*Cel7B	54 ± 5	46 ± 7	0.9 ± 0.1	0.8 ± 0.1	1.71 ± 0.04
	*Th*Cel7A	63 ± 2	37 ± 4	1.51 ± 0.03	0.9 ± 0.1	2.4 ± 0.1
	*Th*Cel7A + *Th*Cel7B	92 ± 8	8 ± 9	5.4 ± 0.2	0.4 ± 0.4	5.8 ± 0.3
Bacterial cellulose	*Th*Cel7B	28 ± 10	72 ± 13	0.8 ± 0.3	1.9 ± 0.3	2.7 ± 0.1
	*Th*Cel7A	71 ± 8	29 ± 8	3.1 ± 0.3	1.3 ± 0.3	4.4 ± 0.1
	*Th*Cel7A + *Th*Cel7B	91 ± 4	9 ± 4	7.5 ± 0.3	0.8 ± 0.3	8.2 ± 0.1

Hydrolysis were carried out at pH 5 for 24 h

the absence of EGs, the intrinsic processivity of the CBH *Th*Cel7A is limited by the nature of a substrate (Kurasin and Väljamäe 2011). The loss of catalytic efficiency is associated with the CBHs getting stuck at the obstacles or at the amorphous regions of the substrate, and being unable to rapidly dissociate and re-engage in the substrate hydrolysis. This leads to a slow dissociation rate and to stalling of Cel7A activity (Kurasin and Väljamäe 2011; Jalak et al. 2012). However, EGs can recognize and cleave amorphous regions of the cellulose chains, leading to release of stuck CBHs. For this reason, a combination of both enzymes is more efficient in terms of soluble sugars release than the sum of the individual activities of the independent enzymes (Nidetzky et al. 1994; Väljamäe et al. 1999; Boisset et al. 2000; Ganner et al. 2012). It is important to notice that total substrate consumption was below 10% under all studied conditions (Table 1).

Notably, both *Th*Cel7A and *Th*Cel7B, while acting separately, effectively stop producing soluble sugars after hydrolyzing cellulosic substrates for 36 h (Fig. 2a). The enzymatic hydrolysis reaches its maximum despite of a large number of available insoluble reducing ends (Fig. 2a and Table 1). This fact is consistent with a limited processivity of *Th*Cel7B, while for the processive *Th*Cel7A, the large number of cellulose chain ends left in the substrate after prolonged incubation indicate that they must be hindered, so that *Th*Cel7A is unable to recognize the termini and to processively hydrolyze the cellulosic chains starting from this point.

As observed in our experiments, when the enzymes are acting in combination, the *Th*Cel7B endoglucanase activity enhances efficiency of *Th*Cel7A, leading to a considerable decrease in the available non-soluble reducing ends as a result of the joint action of the two enzymes. Soluble sugars released from both FP and BC become comparable, reaching 92 ± 8% and 91 ± 4%, respectively (Table 1). This is consistent with the notion of *Th*Cel7B efficiently rescuing stalled *Th*Cel7A in both studied cellulosic substrates and allowing it to access essentially all the available cellulosic termini.

Although the combined action of *Th*Cel7A and *Th*Cel7B virtually exhausts all the available reducing ends in the insoluble cellulosic substrates, the yields of enzymatic hydrolysis from FP and BC are significantly different (Fig. 2a). Since the amounts of the enzymes used for hydrolysis of these two cellulosic substrates were the same, the difference in their enzymatic hydrolysis yields could only depend on the substrates physical and chemical properties and composition. DP_N of BC is higher than that of FP and this limits the obstacle-free path of cellulases in the later substrate (Kurasin and Väljamäe 2011; Jalak et al. 2012). However, based on the analysis of the hydrolytic products, a mixture of *Th*Cel7B and *Th*Cel7As is able to consume virtually all the reducing ends both enzymes are able to generate in the studied substrates (BC and FP). To evaluate if the differences in crystallinity of the substrates could be responsible for the observed enzymatic yields, the crystallinity indices of BC and FP samples were experimentally determined from XDR measurements. Using this technique, the experimentally determined CrI of BC was just slightly higher than that of FP (0.75 and 0.72, respectively). Somewhat higher
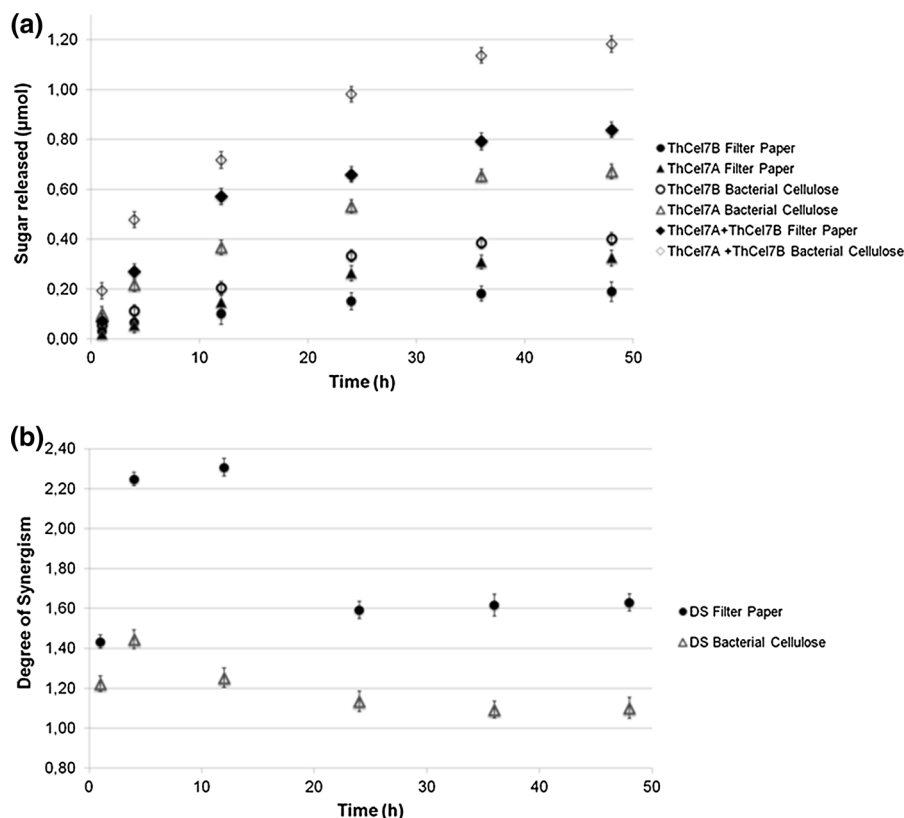
Fig. 2 a Reducing ends (as glucose equivalents) released by *Th*Cel7B and *Th*Cel7A from FP and BC as a function of the hydrolysis time. The experiment was conducteed at pH = 5 and a total amount of reducing ends (soluble from the supernatant + insoluble from the residual substrate) was measured. **b** Degree of synergism (DS) of *Th*Cel7B and *Th*Cel7A calculated for both substrates as a function of the hydrolysis time

crystallinity of BC could indicate that FP might be more susceptible to enzymatic degradation. This is clearly not the case (Fig. 2), which demonstrates that overall crystallinity is not a prime factor in enzymatic hydrolysis of the cellulosic substrates by the cellulase mixtures (Bernardinelli et al. 2015).

*Th*Cel7A/*Th*Cel7B combined activity as a function of pH

Given a difference in optimal pHs between *Th*Cel7A and *Th*Cel7B (Colussi et al. 2011; Pellegrini et al. 2015), the influence of pH on the synergistic action of *Th*Cel7A and *Th*Cel7B during FP hydrolysis was evaluated in the pH range from 3 to 5. The glucose released (in μmol) separately or in combination by the enzymes is presented in Fig. 1b. Saccarification experiments were not carried out at pH values higher than 5 or lower than 3, since both enzymes have low

activities beyond this pH range. Both the synergistic effect and the hydrolysis yield are stronger at pH 5, reaching 0.6 μmol of released glucose. The degree of synergism (DS) at a specific pH was, respectively, 1.14 and 1.33 for pH 4 and pH 5 after 24 h of reaction.

Although the optimal pH for *Th*Cel7B action is pH 3 (Pellegrini et al. 2015), the observed synergism at this pH is very small and DS value can not be reliably determined, because *Th*Cel7A has a very limited enzymatic activity at this pH. At pH 4, the two enzymes together produce ca. 144% more sugar as compared to the *Th*Cel7B hydrolysis alone, and ca. 116% when compared to *Th*Cel7A activity alone. At pH 5, the combined effect is even higher, representing an increase of ca. 124% when compared to the *Th*Cel7A alone and of ca. 228% when compared to the *Th*Cel7B activity alone. This is consistent with the previous studies that show decrease in synergism

between cellulases as the substrate becomes more recalcitrant and the amorphous fraction is preferentially removed (Väljamäe et al. 1999; Jeoh et al. 2006).

These results indicate that the pH effect on the overall activity and synergy between the GH7 cellulases is mainly mediated by the increase in the *Th*Cel7A activity at pH 5 (Fig. 1b). In fact, the slight decrease in *Th*Cel7B activity as a function of pH was completely overwhelmed by the increase in *Th*Cel7A hydrolytic activity, which seems to be a dominant factor for the observed increase in the highly pH-dependent catalytic activity of these two enzymes and their synergy.

*Th*Cel7A/*Th*Cel7B hydrolysis of FP and BC as a function of time

There is a considerable variation in cellulase activities on different substrates, hence the importance of their analysis using various substrates (Kari et al. 2014). Figure 2a shows that the hydrolysis yield is higher for both *Th*Cel7A and *Th*Cel7B acting on BC as compared to FP, thus demonstrating that BC is a more hydrolysable substrate than FP. These cellulose substrates have distinct properties, including the degree of polymerization and the crystallinity, the total surface area available for hydrolysis, and a different morphology, with BC being formed by more homogeneous and thinner fibers, as compared to FP (Kostylev and Wilson, 2012). In Fig. 2b, the DS for *Th*Cel7A and *Th*Cel7B cooperative action using FP and BC substrates is presented as a function of time. These results show that the DS between *Th*Cel7A and *Th*Cel7B differs according to the substrate nature and is higher for FP than for BC. Furthermore, it is clear that for both substrates the synergy is stronger at the beginning of the reaction and steadily decreases with time, since the calculated DS varies during the course of hydrolysis and is higher for shorter hydrolysis times (Fig. 2b). Since, consistently with previous studies (Luterbacher et al. 2015; Payne et al. 2015), enzymatic activity, processivity and degree of synergism between the GH7 cellulases clearly depend on the nature of a particular cellulosic substrate,, investigations of the morphological chances introduced in the substrates by the cellulase hydrolysis were performed using FESEM technique.

FESEM analysis

Changes in the FP morphology introduced by the cellulase activities

To investigate in detail the microscopic morphological changes promoted by *Th*Cel7A and *Th*Cel7B action in FP, FESEM analyses were carried out after 0, 24 and 48 h of hydrolysis of the substrate at pH 5.0 (Fig. 3).

Prior to enzymatic hydrolysis, filter paper structure reveals a set of closely packed fibers, formed by thicker fibers, with external mean diameter between 10 and 30 μm (as the one indicated by the white arrow in Fig. 3a), immersed in a compact solid formed by the thinner microfibrils (mean diameter ca. 0.05 μm), which is indicated by a black arrow (Fig. 3a). The continuous tissue in FP structure is probably formed by cellulose microfibrils detached from the outermost layers of the cotton fibers (thicker fibers in Fig. 3) during FP production.

After 48 h of enzymatic hydrolysis by either the CBH *Th*Cel7A (Fig. 3b) or the EG *Th*Cel7B (Fig. 3c), the FP acquires a more open structure, with larger pores. One can observe that the thinner microfibrils that were previously filling the interstices among the thicker fibers, were preferentially hydrolyzed by the enzymes, leaving voids. It is important to notice that a large number of images were analyzed in these samples (ca. 20 images per duplicate in different regions of each sample) to assure their morphological profile and to prevent local atypical variations in morphology to be taken as a result of hydrolysis. The combined effect of *Th*Cel7A and *Th*Cel7B is very clear in Fig. 3d, where the hydrolysis action is much more pronounced than in samples undergoing hydrolysis with the individual enzymes. After the synergistic action of the two enzymes, basically only the thicker fibers remained in the samples and the mechanical resistance of the enzymatically hydrolyzed paper has been drastically reduced, as observed during handling of samples. An estimative of the total percentage of surface area occupied by voids in each of these samples confirmed the visual observations. In control sample, voids occupy 4–8% of the surface area, while the remaining fraction is filled with the thick fibers or the tissue of thin fibrils. After hydrolysis with *Th*Cel7A for 48 h, the voids represent 9–13% of the total area, and after *Th*Cel7B they
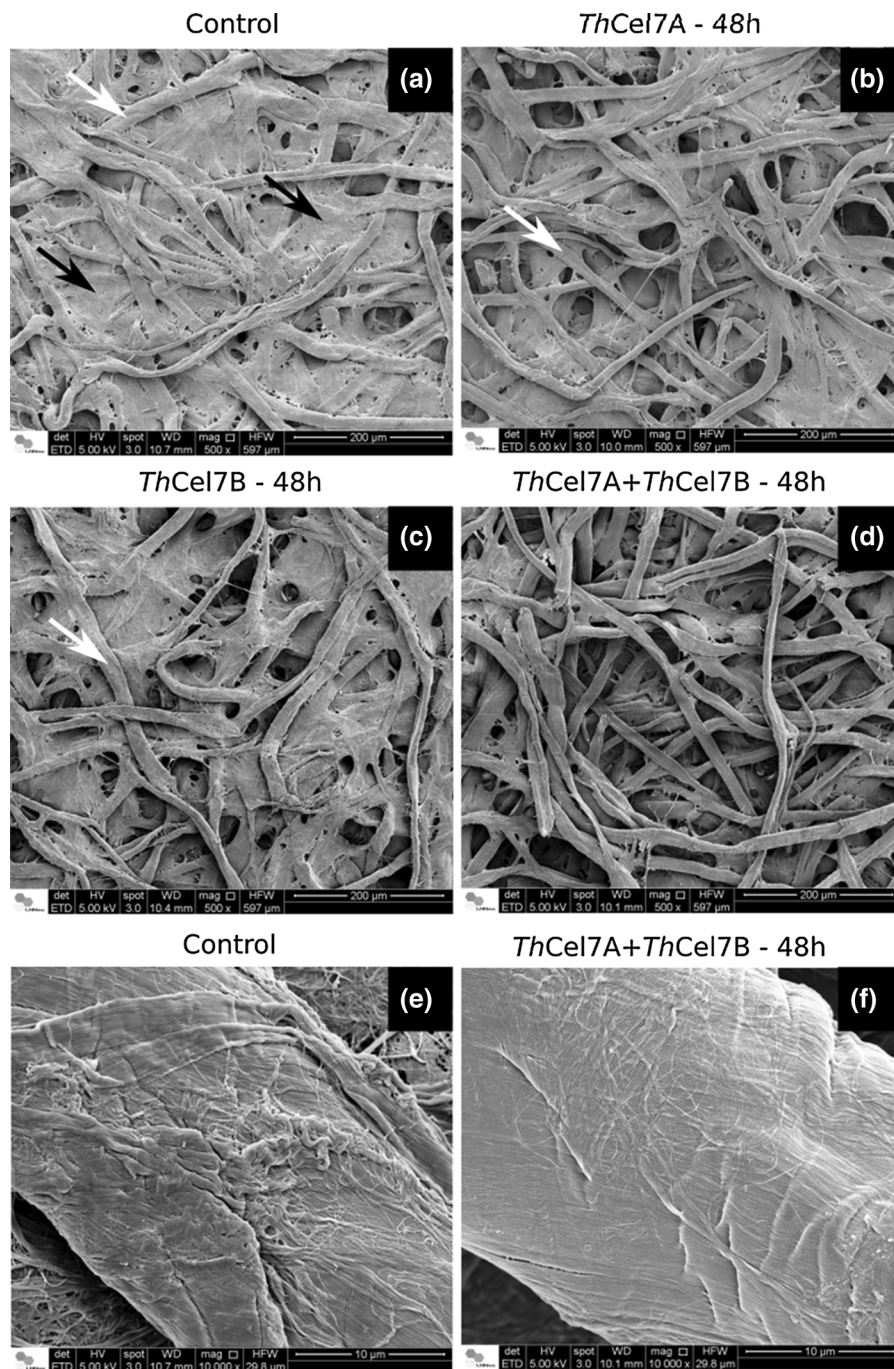
Control   ThCel7A - 48h

ThCel7B - 48h   ThCel7A+ThCel7B - 48h

Control   ThCel7A+ThCel7B - 48h

Fig. 3 FESEM images obtained on filter paper surface: **a**, **e** control and FP after 48 h of hydrolysis (T = 50 °C and pH = 5.0) with **b** CBH ThCel7A; **c** EG ThCel7B; **d**, **f** mixture of ThCel7A and ThCel7B. White arrows indicate thicker fibers, which persist after hydrolysis, and a black arrow in a indicates the mass of thinner microfibrils that are firstly consumed. Scale bar: 200 μm in (**a**–**d**) and 10 μm (**e**, **f**)

occupy 16 to 22% of the total area. Finally, after the synergistic action of ThCel7A and ThCel7B for 48 h, the area occupied by voids represents 20–37%.

Figure 3e, f show amplified areas on thicker fibers of FP before and after 48 h of hydrolysis with ThCel7A and ThCel7B, respectively. Comparing the

images, it is possible to observe that the surface of the remaining thicker fibers that resisted to hydrolysis tends to become smoother after the enzyme action. This effect is more clearly observed in the samples submitted to the joint action of the two enzymes.

The morphological effects caused by enzymatic hydrolysis after reaction times shorter than 24 h are less clear. In addition, the differences between the samples hydrolyzed for 24 or 48 h are almost indistinguishable, as expected considering similar amounts of glucose released by the enzymes at 24 and 48 h (Fig. 2). In spite of this, in some areas of the FP samples hydrolyzed for 24 h, it is possible to find intermediate structural features, showing the ongoing degradation of the thinner fibrils, as indicated by the arrow in Fig. 4a.

Figure 4b shows an area of a similar FP sample after 48 h of hydrolysis, with the thinner microfibrils being all consumed, just as shown in Fig. 3d. When the thin fibrils are degraded or almost degraded, the hydrolysis slows down. The thick fibers are more recalcitrant, and this may be one of the important factors determining the hydrolysis profile of FP, such as observed in Figure ESM1.

Changes in BC morphology introduced by the individual cellulases and their mixture

Solid samples of BC before and after hydrolysis with *Th*Cel7A and *Th*Cel7B alone an a mixture of the two enzymes were also characterized by FESEM. Figure 5 shows FESEM images of bacterial cellulose before (Fig. 5a) and after 48 h of hydrolysis at 50° C and pH = 5.0 with separately *Th*Cel7A (Fig. 5b) and *Th*Cel7B (Fig. 5c) and with both enzymes together (Fig. 5d). It also presents images obtained in the same substrate after 12 h of hydrolysis, using *Th*Cel7B (Fig. 5e) and a mixture of both enzymes (Fig. 5f). The morphology formed by intertwined and well-defined microfibrils in BC before the enzymatic treatment is little changed after the CBH action, except by the appearance of non-fibrilar regions, such as the ones indicated by the arrows in Fig. 5b. These regions could be formed by re-arrangement of BC due to *Th*Cel7A action or they could be already present in the untreated sample and were just being revealed during hydrolysis, by removal of theexternal sample layers. Further, a careful observation of a large number of samples treated with this enzyme by 48 h reveals that the BC fibril network is somewhat more open, similar to what is observed in the FP samples after *Th*Cel7A hydrolysis.

After the action of the EG *Th*Cel7B alone, the BC microfibrils partially lose their shape and appear to be blended with the neighboring fibrils (Fig. 5c). On the other hand, the surface of the BC sample after the synergistic action of *Th*Cel7A and *Th*Cel7B (Fig. 5d) show more distinct microfibrils, without the blending effect observed in Fig. 5c.

A visible reduction in the microfibril diameter could not be observed in the FESEM images of these samples, probably because changes in the microfibrils´ diameters are too small to be detected by this tecnique. More sensitive microscopy tecniques, such
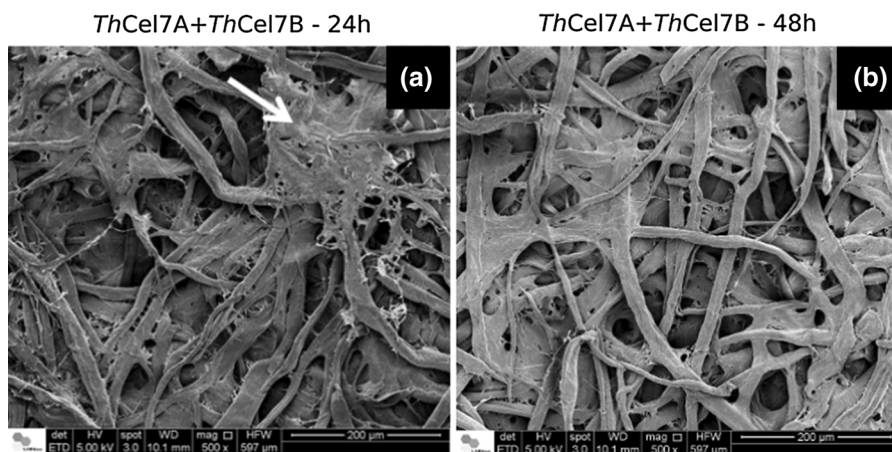

*Th*Cel7A+*Th*Cel7B - 24h   *Th*Cel7A+*Th*Cel7B - 48h

Fig. 4 FESEM images obtained from FP surface after enzymatic hydrolysis (T = 50 °C and pH = 5.0) with a mixture of *Th*Cel7A and *Th*Cel7B for **a** 24 h and **b** 48 h. The arrow indicates the ongoing degradation of the thinner fibrils. Scale bar: 200 μm
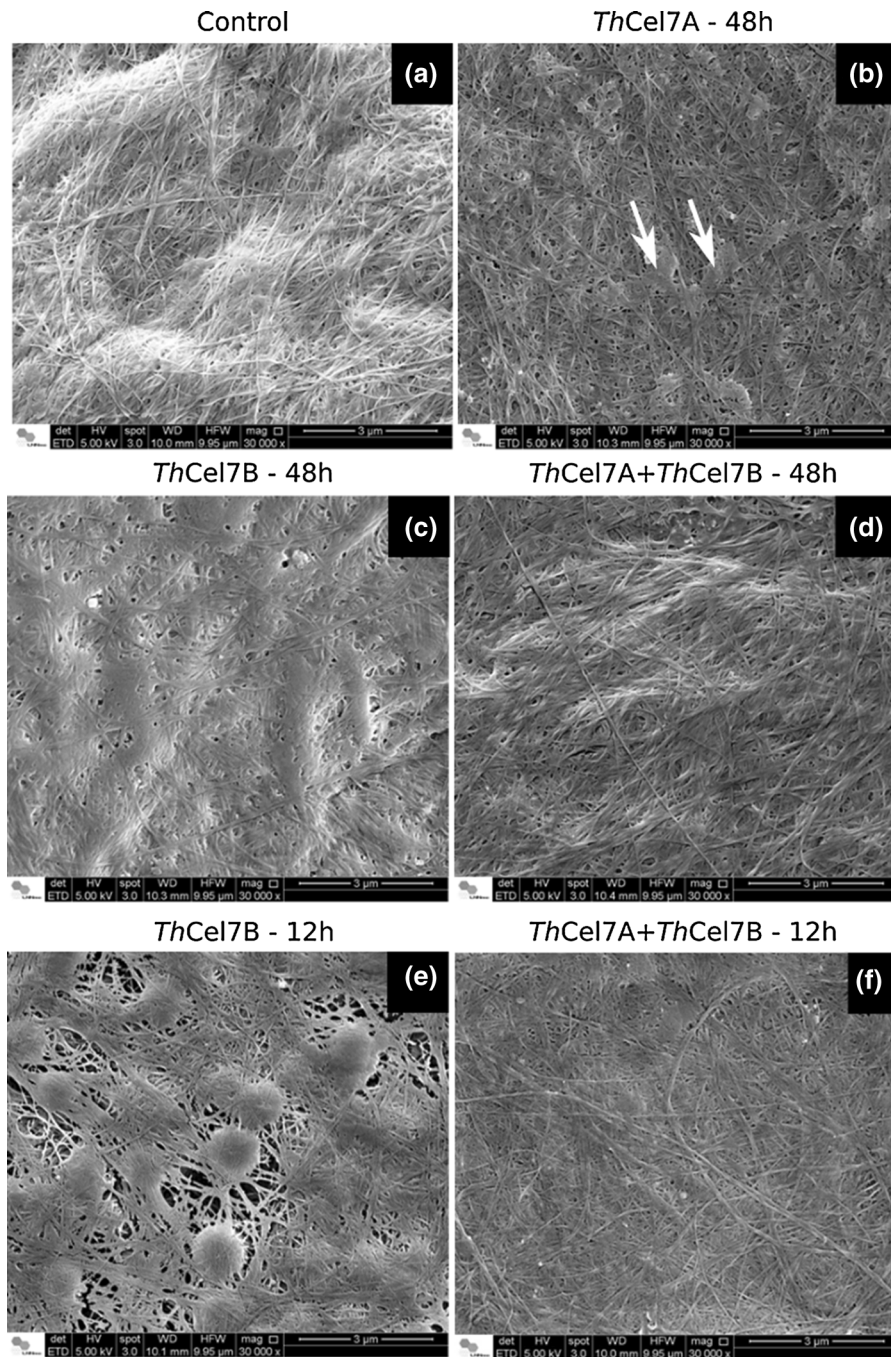
Control

*Th*Cel7A - 48h

*Th*Cel7B - 48h

*Th*Cel7A+*Th*Cel7B - 48h

*Th*Cel7B - 12h

*Th*Cel7A+*Th*Cel7B - 12h

Fig. 5 FESEM images obtained in bacterial cellulose: control (**a**) and BC after hydrolysis (50 °C and pH = 5.0) with **b** *Th*Cel7A; **c**, **e** *Th*Cel7B and **d**, **f** a mixture of *Th*Cel7A and *Th*Cel7B. Hydrolysis times were 48 h in (**a**–**d**) and 12 h in (**e**, **f**). In (**b**), arrows indicate non-fibrilar regions. Scale bar: 3 μm

as atomic force microscopy, could be used for this purpose. Besides, it is possible that a possible diameter reduction effect is being masked by the microfibril swelling prior to drying. However, Fig. 5c

shows a poorer definition of the cellulose microfibril contour, which indicates the presence of hydrolysed material attached to the surface. Furthermore, one would expect that in the more uniform BC, ablative

action of a mixture of *Th*Cel7 and *Th*Cel7B will almost uniformly wear out the surface layers of the sample, resulting in its depolymerization and partial dissolution, thus exposing inner layers of BC microfibrils.

Following the morphological changes induced by enzymatic hydrolysis as a function of time, a very similar tendency is observed. Figure ESM2 shows FESEM images obtained on BC before and after 12 h of hydrolysis at 50 °C and pH = 5.0, using *Th*Cel7A (Figure ESM2). Hydrolysis times of 12 and 48 h can be compared in Figs. 5 and ESM1. Shorter hydrolysis times could not be evaluated, since the morphological changes are too small to be noticed.The typical morphology of a BC surface before the enzymatic treatment, formed by intertwined and well-defined microfibrils, is shown in Figure ESM2a. Non-fibrillar regions can be occasionally found on the untreated sample surface, such as the one indicated by the black arrow in Figure ESM2a. It reinforces the above-mentioned possibility that the cellulase action may be creating some of these non-fibrillar areas, but also could simply unveiling such spots previously existent in the sample. In this case, *Th*Cel7B would be removing sample amorphous regions, revealing a new surface that is a better substrate for the other enzyme (Badino et al. 2017). The opening of the fibrils network is not so easily observed in samples hydrolyzed by the EG for 12 h (Figure ESM2b) in comparison to the untreated sample (Figure ESM2a), which is related to the difficulties associated with the very moderate morphological effects after short hydrolysis times.

Figure 5e shows the morphology formed by blended microfibrils, similar to the one already described for the BC samples hydrolyzed for 48 h in Fig. 5c. But this image also shows a peculiar morphology, formed by globular structures with about 1 μm of diameter placed in the fibril internodes. The origin of these globules is not clear yet, but they are typical of samples that underwent EG action, in other words, of samples treated with *Th*Cel7B alone (mainly in 12 h and 48 h) and jointly by the mixture of *Th*Cel7A and *Th*Cel7B after 48 h. Globular structures do not appear in BC samples before enzyme treatment or in samples treated with the CBH alone, and neither in FP samples. Figure 5f shows BC morphology very similar to the one depicted by Fig. 5d, corroborating the hypothesis

that joint action of the two enzymes removes the non-fibrillar chains attached to the cellulose microfibril surface, and also showing that the hydrolysis time (12 or 48 h) do not result in important morphological differences in these samples.

What is a molecular basis of the effects observed? The FESEM images of FP and BC samples undergoing enzymatic hydrolysis by *Th*Cel7A and *Th*Cel7B and their combination revealed different changes introduced by enzymatic hydrolysis in these substrates.

Morphological changes introduce by *Th*Cel7A and *Th*Cel7B in BC are quite distinct. While the *Th*Cel7A action does not greatly change the substrate morphology (Fig. 5b), the action of the EG *Th*Cel7B alone results in microfibril blending and loss of relief (Fig. 5c). This morphological change is probably related to the endoglucanase attack of the defects along the microfibril surface, leading to the formation of cellulosic polymers that remain partially attached to the surface. When the substrate is immersed in liquid, these cellulose fragments assume the form of swollen polymer branches, partially attached to the main cellulose crystalline microfibrils. After drying, this partially hydrolyzed material acts like a polymeric adhesive, joining neighboring cellulose microfibrils glued together by the extensive network of hydrogen bonds.

This hypothesis is corroborated by the biochemical data presented in Table 1, showing a larger percentage of insoluble reducing sugars in samples resulting from *Th*Cel7B than from *Th*Cel7A action. This is also consistent with the processive, abrasive surface action of CBH *Th*Cel7A and the far less processive EG nature of *Th*Cel7B.

Similar effects concerning the softening and the swelling of cellulose fibrils were observed by Wang et al. (2013), who used high-resolution atomic force microscopy to study the degradation of bacterial cellulose obtained from *Acetobacter xylinum* by two exoglucanases (*Tr*Cel6A and *Tr*Cel7A) and an endoglucanase (*Tr*Cel6B) from *Trichoderma reesei*. These authors did not observe effects of the individual action of any of these enzymes on the cellulosic substrate, but they did observe the synergistic effects caused by the enzyme mixtures. The degradation effects were dependent on the addition order of the enzymes: hydrolysis efficiency was higher when the CBH (*Tr*Cel7A) was added to a sample previously

treated with the EG *Tr*Cel7B than when the opposite order was used. According to the authors, the EG action resulted in amorphous cellulose removal and softened and swelled fibrils, with exposed single microfibrils, thus facilitating the following CBH attack (Wang et al. 2013).

Finally, combined action of *Th*Cel7A and *Th*Cel7B on BC reveals more distinct fibers, devoid of the adhesive layers observed in the samples treated by *Th*Cel7B alone (Fig. 5). This presumaby happens because the partially attached amorphous chains (responsible for the gluing effect) were removed by the CBH ablation, which takes advantage of the larger number of chain ends available for hydrolysis and indicates the *Th*Cel7B action as a facilitator to the CBH action. This observation also agrees with the results obtained in our biochemical assays for quantification of soluble and insoluble sugars (Table 1) and ressemble the results obtained with FP undergoing the action of the same enzymes.

In the case of FP, FESEM images reveal that in this more heterogeneous substrate, in which thinner microfibrils and thicker fibers co-exist, both GH7 cellulases preferably hydrolyze the thin, less protected and apparently more disordered microfibrils in interstitial layers first (Fig. 3), while the thicker fibers are significantly more recalcitrant toward enzymatic hydrolysis. Apparently, the thicker fibers are not being significantly modified by individual enzymes, while synergistic action of *Th*Cel7A and *Th*Cel7B preferentially degrade the outermost fiber layers.

The greater accessibility and the preferential consumption of microfibrils instead of the larger cellulose packed blocks was also observed by atomic force microscopy of model cellulosic substrates by Ganner and collaborators (Ganner et al. 2012). This effect can be assigned to a large number of termini accessible to *Th*Cel7A processive hydrolysis, as well as the efficiency with which endo-type enzymatic attacks of *Th*Cel7B and also *Th*Cel7A create new cuts in the thin interstitial fibrils.

It is known that the substrate morphology has a strong effect on the efficiency of enzymatic hydrolysis of plant-derived substrates and polymers (Zhang and Lynd 2004; Rezende et al. 2011). Both BC and FP are cellulosic substrates made out of fibrils. The FP is much less homogenous, being composed by thick hollow cotton fibers with an external average diameter (d) of about 16 ± 5 μm (Fig. 3e, f) and

walls of about 2–4 μm thick (Ververis et al. 2004), joined together by a thinner, less structured material filling in voids between the fibers (Fig. 3a). On the other hand, BC is composed by a large number of much thinner and much more homogeneous microfibrils with an average diameter of about 0.05 μm. Chemically, these two cellulosic materials are very similar. Why then are their enzymatic hydrolysis yields so different? We argue that the main reason is their considerably different surface-to-volume ratio.

Consider first an object of a cylindrical shape. Since volume of a cylinder is

$$V_c = \frac{1}{4}\pi d^2 L \qquad (1)$$

and its surface area can be calculated as

$$S_c = \pi d L, \qquad (2)$$

the surface-to-volume ratio decreases as *4/d* with the increase in a cylinder diameter. This means that cellulose "packed" in thick fibers has smaller surface area as opposed to the very same mass of cellulose presented in the form of thin microfibrils. The surface area decreases inversely proportional to the increase in the average diameter of a typical fiber (or fibril), provided that the fibers are separated. The same size effect is well-known for colloidal systems and nanoparticles (Hunter 2001; Goodwin 2004). In the case of the hollow tubes, such as coton fibers, a volume of the tube can be calculated as

$$V_t = \frac{1}{4}\pi \left(d_{out}^2 - d_{inn}^2 \right) L \qquad (3)$$

where d_{out} and d_{inn} are outer and inner diameter of the tube, respectively.

The surface area of the long tube be calculated as

$$S_t = \pi(d_{out} + d_{inn})L \qquad (4)$$

Thus, the surface to volume ratio for a tube-like object can be estimated as

$$S_t/V_t = 4/(d_{out} - d_{inn}) \sim 4/t \qquad (5)$$

where t is a thickness of the tube wall.

Therefore, accessible surface area of the same unit of volume (or mass) decreases as d/t (microfibril diameter to cell wall thickness) as the microfibrils pack into thicker cell walls.

Efficiency of enzymatic attack of cellulosic substrates strongly depends on their accessible surface

area. This explains why never dried cellulose fibers are so susceptible to enzymatic degradation by cellulases. Drying leads to irreversible aggregation of BC fibrils and substantial decrease of their surface area, however, the resulting material never gets as dense and organized as cellulose fibers or cotton cell walls. Much thicker FP cellulose fibers provide considerably smaller accessible surface area as compared to the much thinner interstitial microfibrils. This leads to a preferential degradation of the fine interstitial material between the thick fibers of the FP and "polishing" of the thick fiber surfaces. When the cellulases exhaust all possible cleavage sites on the surfaces of fibers, their hydrolytic activities stall. Even taking into account hornification, two orders of magnitude difference in the diameters of FP fibers and BC microfibrils make a large difference in accessibility of the average cellulose chain within these substrates leading to much more efficient and rapid consumption of BC by cellulases.

Combined enzymatic action of the CBHs and the EGs on FP is mostly limited to the consumption of the thin interstitial microfibrils and to removing inhomogeneous external layers from the thick fibers, which however mostly stay intact (Fig. 3e, d). As judged from our FESEM analysis, the average cross-section of the FP fibers remains practically the same after enzymatic attack. The mean apparent diameter of thick FP cotton fibers, which was 16.4 ± 5.4 µm in the control sample, is virtually unchanged (16.5 ± 5.5 µm) after 48 h of hydrolysis with the two enzymes acting synergistically. These average diameter values were obtained by measuring 250 and 270 fibers in 5 different regions of the control sample and of the sample after ThCel7A + ThCel7B hydrolysis for 48 h, respectively.

In this context, additional enzymatic activities leading to unstructuring of the cellulose fibers such as expansins (Arantes and Saddler 2010; Tomazini et al. 2015) and oxidative enzymes (e.g., LPMOs) capable of introducing oxidation nicks in the cellulase chains at the surface of the fibrils would have a significant boosting effect on the enzymatic hydrolysis of cellulosic substrates (Vaaje-Kolstad et al. 2010; Horn et al. 2012; Payne et al. 2015).

Due the importance of synergic action of EG and CBH in cellulose hydrolysis, here the action of two GH7 cellulases, ThCel7B and ThCel7A, on two different cellulosic substrates was studied for the first time, by following soluble and insoluble products of their hydrolysis and by analysing changes in the morphology of the substrates. The hydrolytic yields and ratios between soluble and insoluble products generation varied with the substrate being considerably different for ThCel7A, ThCel7B and their combination. Our FESEM studies reveal that enzymes introduced morphological changes in BC are quite uniform, whereas during FP hydrolysis the enzymes specifically attack thin interstitial microfibrils, leaving thick fibers almost intact. This behavior has a direct impact on efficiency of enzymatic hydrolysis, resulting in higher yields from BC than from FP for the same enzymatic dose. Our findings, obtained with model cellulosic substrates FP and BC, might assist in improvements of plant biomass pretreatments and optimization of enzymatic mixtures for its efficent depolymerization, although the challenges due to the complexity of real lignocellulosic substrates can not be ignored.

Conclusions

The synergistic effects between ThCel7B and ThCel7A are pH-dependent and governed by ThCel7A optimal pH. For both FP and BC, a joint action of the cellulases leads to a release of almost exclusively soluble products and exhaustion of the available cleavage sites within the insoluble substrates, although their hydrolytic yields are considerably different. We argue that the main reason for differences in saccharification efficiencies reside in a size effect: thicker FP fibers have significantly smaller surface areas accessible to cellulases, which make them significantly more recalcitrant.

Compliance with ethical standards

Conflict of interest The authors declare that they have no competing interests.

References

Arantes V, Saddler J (2010) Access to cellulose limits the efficiency of enzymatic hydrolysis: the role of amorphogenesis. Biotechnol Biofuels 3:4. https://doi.org/10.1186/1754-6834-3-4

Badino SF, Christensen SJ, Kari J, Windahl MS, Hvidt S, Borch K, Westh P (2017) Exo–exo synergy between Cel6A and Cel7A from *Hypocrea jecorina*: role of carbohydrate binding module and the endo-lytic character of the enzymes. Biotechnol Bioeng 114:1639–1647. https://doi.org/10.1002/bit.26276

Bernardinelli OD, Lima MA, Rezende CA, Polikarpov I, deAzevedo ER (2015) Quantitative 13C MultiCP solid-state NMR as a tool for evaluation of cellulose crystallinity index measured directly inside sugarcane biomass. Biotechnol Biofuels 8:110. https://doi.org/10.1186/s13068-015-0292-1

Boisset C, Fraschini C, Schülein M, Henrissat B, Chanzy H (2000) Imaging the enzymatic digestion of bacterial cellulose ribbons reveals the endo character of the cellobiohydrolase Cel6A from *Humicola insolens* and its mode of synergy with cellobiohydrolase Cel7A. Appl Environ Microbiol 66:1444–1452. https://doi.org/10.1128/aem.66.4.1444-1452.2000

Boisset C, Pétrequin C, Chanzy H, Henrissat B, Schülein M (2001) Optimized mixtures of recombinant *Humicola insolens* cellulases for the biodegradation of crystalline cellulose. Biotechnol Bioeng 72:339–345. https://doi.org/10.1002/1097-0290(20010205)72:3<339::AID-BIT11>3.0.CO;2-%23

Chawla PR, Bajaj IB, Survase SA, Singhal RS (2009) Microbial cellulose: fermentative production and applications. Food Technol Biotechnol 47:107–124

Colussi F, Serpa V, Delabona PS, Manzine LR, Voltatodio ML, Alves R, Mello BL, Pereira N Jr, Farinas CS, Golubev AM, Santos MA, Polikarpov I (2011) Purification, and biochemical and biophysical characterization of cellobiohydrolase I from *Trichoderma harzianum* IOC 3844. J Microbiol Biotechnol 21:808–817. https://doi.org/10.4014/jmb.1010.10037

Cruys-Bagger N, Tatsumi H, Ren GR, Borch K, Westh P (2013) Transient kinetics and rate-limiting steps for the processive cellobiohydrolase Cel7: effects of substrate structure and carbohydrate binding domain. Biochemistry 52:8938–8948. https://doi.org/10.1021/bi401210n

Ganner T, Bubner P, Eibinger M, Mayrhofer C, Plank H, Nidetzky B (2012) Dissecting and reconstructing synergism: in situ visualization of cooperativity among cellulases. J Biol Chem 287:43215–43222. https://doi.org/10.1074/jbc.M112.419952

Goodwin JW (2004) Colloids and Interfaces with surfactants and polymers—an introduction. Wiley, London. https://doi.org/10.1002/0470093919

Harris P, Welner D, McFarland K, Re E, Navarro Poulsen J, Brown K, Salbo R, Ding H, Vlasenko E, Merino S (2010) Stimulation of lignocellulosic biomass hydrolysis by proteins of glycoside hydrolase family 61: structure and function of a large, enigmatic family. Biochemistry 49:3305–3316. https://doi.org/10.1021/bi100009p

Hemsworth GR, Johnston EM, Davies GJ, Walton PH (2015) Lytic polysaccharide monooxygenases in biomass conversion. Trends Biotechnol 33:747–761. https://doi.org/10.1016/j.tibtech.2015.09.006

Henrissat B, Driguez H, Viet C, Schulein M (1985) Synergism of cellulases from *Trichoderma reesei* in the degradation of cellulose. Nat Biotechnol 3:722–726. https://doi.org/10.1038/nbt0885-722

Horn SJ, Vaaje-Kolstad G, Westereng B, Eijsink VGH (2012) Novel enzymes for the degradation of cellulose. Biotechnol Biofuels 5:1–13. https://doi.org/10.1186/1754-6834-5-45

Hunter RJ (2001) Foundations of colloid science, 2nd edn. Oxford University Press, Oxford

Igarashi K, Uchihashi T, Koivula A, Wada M, Kimura S, Okamoto T, Penttilä M, Ando T, Samejima M (2011) Traffic jams reduce hydrolytic efficiency of cellulase on cellulose surface. Science 333:1279–1282. https://doi.org/10.1126/science.l208386

Jalak J, Kurašin M, Teugjas H, Väljamäe P (2012) Endo-exo synergism in cellulose hydrolysis revisited. J Biol Chem 287:28802–28815. https://doi.org/10.1074/jbc.M112.381624

Jeoh T, Wilson DB, Walker LP (2006) Effect of cellulase mole fraction and cellulose recalcitrance on synergism in cellulose hydrolysis and binding. Biotechnol Prog 22:270–277. https://doi.org/10.1021/bp050266f

Kari J, Olsen J, Borch K, Cruys-Bagger N, Jensen K, Westh P (2014) Kinetics of cellobiohydrolase (Cel7A) variants with lowered substrate affinity. J Biol Chem 47:32459–32468. https://doi.org/10.1074/jbc.M114.604264

Katzen F (2007) Gateway® recombinational cloning: a biological operating system. Exp Opin Drug Discov 2:571–589. https://doi.org/10.1517/17460441.2.4.571

Kostylev M, Wilson DB (2012) Synergistic interactions in cellulose hydrolysis. Biofuels 3:61–70. https://doi.org/10.4155/bfs.11.150

Kostylev M, Wilson D (2014) A distinct model of synergism between a processive endocellulase (*Tf*Cel9A) and an exocellulase (*Tf*Cel48A) from *Thermobifida fusca*. Appl Environ Microbiol 80:339–344. https://doi.org/10.1128/AEM.02706-13

Kurasin M, Väljamäe P (2011) Processivity of cellobiohydrolases is limited by the substrate. J Biol Chem 286:169–177. https://doi.org/10.1074/jbc.M110.161059

Kuusk S, Sørlie M, Väljamäe P (2015) The predominant molecular state of bound enzyme determines the strength and type of product inhibition in the hydrolysis of recalcitrant polysaccharides by processive enzymes. J Biol Chem 290:11678–11691. https://doi.org/10.1074/jbc.M114.635631

Li Y, Irwin DC, Wilson DB (2007) Processivity, substrate binding, and mechanism of cellulose hydrolysis by *Thermobifida fusca* Cel9A. Appl Environ Microbiol 73:3165–3172. https://doi.org/10.1128/AEM.02960-06

Luterbacher JS, Moran-Mirabal JM, Burkholder EW, Walker LP (2015) Modeling enzymatic hydrolysis of lignocellulosic substrates using confocal fluorescence microscopy I: filter paper cellulose. Biotechnol Bioeng 112:21–31. https://doi.org/10.1002/bit.25329

Miller G (1959) Use of dinitrosalicylic acid reagent for determination of reducing sugar. Anal Chem 31:426–428. https://doi.org/10.1021/ac60147a030

Nidetzky B, Steiner W, Hayn M, Claeyssens M (1994) Cellulose hydrolysis by the cellulases from *Trichoderma reesei*: a new model for synergistic interaction. Biochem J 298:705–710. https://doi.org/10.1042/bj29880705

Park S, Baker JO, Himmel ME, Parilla PA, Johnson DK (2010) Cellulose crystallinity index: measurement techniques and their impact on interpreting cellulase performance. Biotechnol Biofuels 3:10. https://doi.org/10.1186/1754-6834-3-10

Payne CM, Knott BC, Mayes HB, Hansson H, Himmel ME, Sandgren M, Ståhlberg J, Beckham GT (2015) Fungal cellulases. Chem Rev 115:1308–1448. https://doi.org/10.1021/cr500351c

Pellegrini VO, Serpa VI, Godoy AS, Camilo CM, Bernardes A, Rezende CA, Junior NP, Franco Cairo JP, Squina FM, Polikarpov I (2015) Recombinant *Trichoderma harzianum* endoglucanase I (Cel7B) is a highly acidic and promiscuous carbohydrate-active enzyme. Appl Microbiol Biotechnol 99:9591–9604. https://doi.org/10.1007/s00253-015-6772-1

Reese ET, Siu RGH, Levinson HS (1950) The biological degradation of soluble cellulose derivatives and its relationship to the mechanism of cellulose hydrolysis. J Bacteriol 59:485–497

Rezende CA, Lima MA, Maziero P, de Azevedo ER, Garcia W, Polikarpov I (2011) Chemical and morphological characterization of sugarcane bagasse submitted to a delignification process for enhanced enzymatic digestibility. Biotechnol Biofuels 4:54. https://doi.org/10.1186/1754-6834-4-54

Schneider CA, Rasband WS, Eliceiri KW (2012) NIH Image to ImageJ: 25 years of image analysis. Nat Methods 9:671–675. https://doi.org/10.1038/nmeth.2089

Schramm M, Hestrin S (1954) Synthesis of cellulose by *Acetobacter xylinum*. 1. Micromethod for the determination of celluloses. Biochem J 56:163–166. https://doi.org/10.1042/bj0560163

Serpa VI, Polikarpov I (2011) Enzymes in bioenergy. In: Goldman MSBH (ed) Routes to cellulosic ethanol, 1st edn. Springer, New York, pp 97–113. https://doi.org/10.1007/978-0-387-92740-4_7

Silveira MH, Aguiar RS, Siika-aho M, Ramos LP (2014) Assessment of the enzymatic hydrolysis profile of cellulosic substrates based on reducing sugar release. Bioresour Technol 151:392–396. https://doi.org/10.1016/j.biortech.2013.09.135

Ståhlberg J, Johansson G, Pettersson G (1993) *Trichoderma reesei* has no true exo-cellulase: all intact and truncated cellulases produce new reducing end groups on cellulose. Biochim Biophys Acta 1157:107–113. https://doi.org/10.1016/0304-4165(93)90085-M

Storms R, Zheng Y, Li H, Sillaots S, Martinez-Perez A, Tsang A (2005) Plasmid vectors for protein production, gene expression and molecular manipulations in *Aspergillus niger*. Plasmid 53:191–204. https://doi.org/10.1016/j.plasmid.2004.10.001

Textor LC, Colussi F, Silveira RL, Serpa V, de Mello BL, Muniz JRC, Squina FM, Pereira N, Skaf MS, Polikarpov I (2013) Joint X-ray crystallographic and molecular dynamics study of cellobiohydrolase I from *Trichoderma harzianum*: deciphering the structural features of cellobiohydrolase catalytic activity. FEBS J 280:56–69. https://doi.org/10.1111/febs.12049

Tomazini A, Dolce LG, de Oliveira Neto M, Polikarpov I (2015) *Xanthomonas campestris* expansin-like X domain is a structurally disordered beta-sheet macromolecule capable of synergistically enhancing enzymatic efficiency of cellulose hydrolysis. Biotechnol Lett 37:2419–2426. https://doi.org/10.1007/s10529-015-1927-9

Vaaje-Kolstad G, Westereng B, Horn SJ, Liu ZL, Zhai H, Sørlie M, Eijsink VGH (2010) An oxidative enzyme boosting the enzymatic conversion of recalcitrant polysaccharides. Science 330:219–222. https://doi.org/10.1126/science.1192231

Väljamäe P, Sild V, Nutt A, Pettersson G, Johansson G (1999) Acid hydrolysis of bacterial cellulose reveals different modes of synergistic action between cellobiohydrolase I and endoglucanase I. Eur J Biochem 266:327–334. https://doi.org/10.1046/j.1432-1327.1999.00853.x

Ververis C, Georghiou K, Christodoulakis N, Santas P, Santas R (2004) Fiber dimensions, lignin and cellulose content of various plant materials and their suitability for paper production. Ind Crop Prod 19:245–254. https://doi.org/10.1016/j.indcrop.2003.10.006

Wang T, Park YB, Caporini MA, Rosay M, Zhong L, Cosgrove DJ, Hong M (2013) Sensitivity-enhanced solid-state NMR detection of expansin's target in plant cell walls. PNAS 110:16444–16449. https://doi.org/10.1073/pnas.1316290110

Watson DL, Wilson DB, Walker LP (2002) Synergism in binary mixtures of *Thermobifida fusca* cellulases Cel6B, Cel9A, and Cel5A on BMCC and Avicel. Appl Biochem Biotechnol 101:97–111. https://doi.org/10.1385/ABAB:101:2:097

Wilson DB, Kostylev M (2012) Cellulase processivity. Methods in molecular biology. Methods Mol Biol 908:93–99. https://doi.org/10.1007/978-1-61779-956-3_9

Woodward J, Hayes MK, Lee NE (1988) Hydrolysis of cellulose by saturating and non-saturating concentrations of cellulase: implications for synergism. Nat Biotechnol 6:301–304. https://doi.org/10.1038/nbt0388-301

Zhang YHP, Lynd LR (2004) Toward an aggregated understanding of enzymatic hydrolysis of cellulose: noncomplexed cellulase systems. Biotechnol Bioeng 88:797–824. https://doi.org/10.1002/bit.20282